
Spectroscopy of High-Temperature Solar Flare Plasmas [and Discussion]

K. J. H. Phillips and A. Fludra

Phil. Trans. R. Soc. Lond. A 1991 **336**, 461-470

doi: 10.1098/rsta.1991.0095

Email alerting service

Receive free email alerts when new articles cite this article - sign up in the box at the top right-hand corner of the article or click [here](#)

To subscribe to *Phil. Trans. R. Soc. Lond. A* go to:
<http://rsta.royalsocietypublishing.org/subscriptions>

Spectroscopy of high-temperature solar flare plasmas

BY K. J. H. PHILLIPS

Astrophysics Division, Rutherford Appleton Laboratory, Chilton, Didcot, Oxfordshire OX11 0QX, U.K.

The past decade has seen great improvements in the quality of X-ray spectra of solar flares obtained from spacecraft. Such spectra show lines emitted by highly ionized atoms of abundant elements which make up high-temperature plasma contained within coronal magnetic flux tubes. This plasma is probably energized at or a little before the flare impulsive stage, as revealed by bursts of hard X-rays. Temperature and density conditions can be deduced from ratios of line intensities, as well as element abundances under certain conditions. In this paper, several examples of line ratios to deduce these are given. Analysis shows that there is a wide range of electron temperatures – generally from 2×10^6 K to 20×10^6 K – though sometimes even higher. Electron densities of around 10^{17} – 10^{18} m⁻³ have been derived, higher values occurring at the flare peak or just before, and then declining. The physical conditions of the hot plasma are now precisely enough known from X-ray spectroscopy that models of flares which have been constructed in the past can be constrained. The most profitable direction for research in this area in the near future would in fact appear to be for a much better linking of the findings from X-ray spectra and modelling of plasma in flux tubes to understand better the flare process in general.

1. Introduction

There has been a considerable improvement in the quality of X-ray spectra of active regions and flares in the solar corona in the recent past, and together with improvements in atomic data these spectra are giving much valuable information on the physical nature of the hot plasmas emitting the spectra. The most notable of the instruments obtaining these spectra in this time have been Bragg crystal spectrometers on board the U.S. spacecraft *P78-1* and *Solar Maximum Mission (SMM)* and the Japanese *Hinotori* spacecraft, though X-ray spectra of comparable resolution were also obtained from earlier instruments on the Soviet *Intercosmos* and U.S. *OVI-17* spacecraft.

The wavelength range covered by the totality of these instruments is approximately 0.17–2.5 nm, though some instruments had only limited wavelength ranges designed to include particularly interesting groups of lines. The range as a whole covers many very intense lines, many due to transitions connecting to the ground state of H-like or He-like ionization stages of elements abundant in the Sun, particularly those of even atomic number $Z \leq 26$. There are also numerous lines due to transitions in a wide variety of ionization stages of iron. Dielectronic satellite lines occur in great profusion near the resonance lines of H-like and He-like ion lines of

Phil. Trans. R. Soc. Lond. A (1991) **336**, 461–470

Printed in Great Britain

461

iron, and are also present but weaker in the corresponding stages of calcium, argon and elements of smaller Z .

Many of these lines are rich in diagnostic potential, so are able to give us much information about the emitting plasma. Electron density and temperature can, for example, be determined from line ratios, and under certain circumstances element abundances. In this review, examples of such line ratios will be discussed together with the results. Some future directions for this line of research are suggested.

2. Density-sensitive line ratios

Several line ratios in the soft X-ray region can be used to determine electron density N_e in flares and active regions. One of the most well-known is the ratio of intercombination and forbidden lines in the spectra of He-like ions of relatively low- Z elements. The reason for the density sensitivity is the well-known fact that the 2^3S_1 level is metastable, and at high N_e there is a transfer of its population to the 2^3P term; the intercombination line ($1^1S_0-2^3P_1$) is hence enhanced in intensity, and the forbidden line ($1^1S_0-2^3S_1$) is correspondingly decreased in intensity (see Gabriel & Jordan 1969).

The corresponding lines of He-like neon (Ne^{IX}) are in the range 1.34–1.37 nm. They are of particular interest as they are sensitive to N_e in exactly the range expected for solar flare plasmas, *ca.* 10^{17} – 10^{18} m^{-3} . The lines are emitted at temperatures of *ca.* 4×10^6 K. Though this ion is one of the most interesting for this purpose, the spectral range in which the lines occur unfortunately also contains a large number of Fe^{XIX} lines of the $2p^4-2p^33d$ array, which come up strongly when a flare takes place. Until recently, the wavelengths and intensities of the Fe^{XIX} lines were not well known, but the work of Bhatia *et al.* (1989) has improved the situation. In this work, optimized wavelengths based on the Cowan atomic structure code were combined with distorted-wave collision strengths to give a theoretical Fe^{XIX} line spectrum which was then added to a corresponding Ne^{IX} spectrum. The latter was calculated using R -matrix atomic data from Keenan *et al.* (1987).

The work of Bhatia *et al.* compared observed spectra from the Flat Crystal Spectrometer (FCS) on *SMM* with synthetic spectra based on calculated Ne^{IX} and Fe^{XIX} data. Figure 1 shows the case for a spectrum during the decay stage of a flare on 25 August 1980. An electron density of 2×10^{17} m^{-3} was found to be a good fit to the Ne^{IX} lines. Several such spectra were obtained from the FCS at the peak and part of the decay of a much larger flare on 5 November 1980. The values of N_e are higher at the peak (*ca.* 10^{18} m^{-3}) by a factor of ten than towards the end of the flare (*ca.* 10^{17} m^{-3}). Very similar results were obtained by Doschek *et al.* (1981) for lines of He-like oxygen (O^{VII}), which has a slightly lower temperature of formation than He-like neon. The peak densities from the Ne^{IX} lines imply that the emitting volume viewed by the FCS is in the form of very fine filaments or small spots. This is deduced from the value of the emission measure, $\int_V N_e^2 dV$ (where V is the emitting volume), determined from the absolute line flux, and the fact that the FCS field of view (FWHM) is 14×14 arcsec in angular measure (10^4 km square). If the flare dimension along the line of sight is *ca.* 10^4 km, the flare emitting volume is of the order of only 1% of that viewed by the FCS.

There are density indicators from the intensities of lines at higher temperatures. Lines of the transition arrays $2p^n-2p^{n-1}3d$ in Fe^{XX} ($n = 3$), Fe^{XXI} ($n = 2$) and Fe^{XXII}

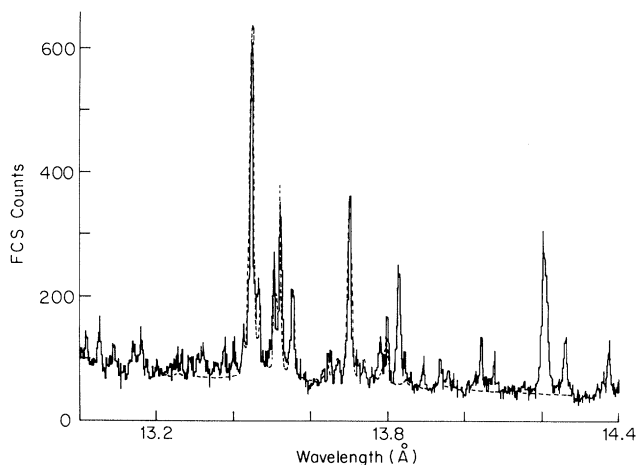


Figure 1. rcs spectrum over the region of the Ne^{IX} lines (1.3447, 1.3553, 1.3699 nm) and Fe^{XIX} lines (histogram). (Unit of wavelength in axis labelling is \AA , where $1 \text{\AA} = 0.1 \text{ nm}$.) The dashed curve is the computer fit based on theoretical Ne^{IX} and Fe^{XIX} line intensities and wavelengths.

($n = 1$) occur at wavelengths of around 1.2 nm. The ground state configurations contain more than one fine-structure level, and, while all the population resides in the ground level at $N_e \lesssim 10^{18} \text{ m}^{-3}$, the other levels begin to be populated if the density is larger. This affects the intensities of lines. The case of two lines, the $\text{Fe}^{\text{XXI}} \text{}^3\text{P}_2\text{-}^3\text{D}_3$ and $\text{Fe}^{\text{XXII}} \text{}^2\text{P}_{3/2}\text{-}^2\text{D}_{5/2}$ lines, are expected to be present only if the electron density N_e is greater than 10^{18} and $3 \times 10^{18} \text{ m}^{-3}$ respectively. These lines are expected to occur at wavelengths of about 1.232 nm and 1.1921 nm. Neither is present in a spectrum obtained during the decay phase of a flare on 25 August 1980, thus placing an upper limit of 10^{18} m^{-3} for the electron density. These upper limits are compatible with the Ne^{IX} results already mentioned, which indicate electron densities of about 10^{17} m^{-3} during the decay of flares. Unfortunately, the spectral region containing the Fe^{XXI} and Fe^{XXII} lines was not scanned again by the rcs during the lifetime of *SMM* owing to an early failure of the channel viewing this range, so further analysis was not possible.

Inner-shell lines due to transitions of the type $1s^2 2s^2 2p^n\text{-}1s 2s^2 2p^{n+1}$ in Fe^{XIX} , Fe^{XX} and Fe^{XXI} are also density dependent. To a first approximation, lines from each ion occur in discrete groups of satellite lines with increasing wavelength (Fe^{XIX} at *ca.* 0.1915, Fe^{XX} at *ca.* 0.1905, Fe^{XXI} at *ca.* 0.1895 nm), all on the long-wavelength side of the resonance line ($1s^2 1\text{S}_0\text{-}1s 2p^1\text{P}_1$) at 0.1850 nm of He-like iron (Fe^{XXV}) and the satellite lines of $\text{Fe}^{\text{XXII}}\text{-Fe}^{\text{XXIV}}$. Dielectronic recombination is the most important excitation process for the $\text{Fe}^{\text{XIX}}\text{-Fe}^{\text{XXI}}$ and indeed nearly all the other satellites. Thus, the Fe^{XX} lines are excited by the dielectronic recombination of the Fe^{+20} ion. As already indicated, this ion has several fine structure levels within its ground configuration ($1s^2 2s^2 2p^2$), and all may be significantly populated if N_e is larger than about 10^{18} m^{-3} . Since dielectronic recombination can proceed from any of these levels, the pattern of Fe^{XX} lines formed by dielectronic excitation is density-dependent. In a study of such lines due to $\text{Fe}^{\text{XIX}}\text{-Fe}^{\text{XXI}}$ by Phillips *et al.* (1983), calculated line intensities were compared with observed values during solar flares as seen by the Bent Crystal Spectrometer (BCS) on *SMM* and the SOLFLEX spectrometer, and it was found that nearly all spectra were compatible with the low-density limit

$N_e < 10^{18} \text{ m}^{-3}$. Such spectra were observed in the decay stages of flares when these lines are most apparent: at earlier stages in flares, the lines are hardly visible above the instrumentally formed background radiation. This result thus confirms that from the FCS observations mentioned earlier. The predicted change in the pattern of lines at higher N_e was confirmed by Phillips *et al.* through a comparison of calculated and observed spectra from plasma produced in the Princeton Large Torus, for which $N_e \approx 2 \times 10^{20} \text{ m}^{-3}$.

3. Temperature-sensitive line ratios

The number of useful density-sensitive line ratios in solar-flare X-ray spectra is not large, but by contrast there are several that are sensitive to electron temperature (T_e). The most well known are the satellite lines due to the Li-like stage on the long-wavelength side of the He-like resonance line in elements with atomic number $Z \geq 12$. Those satellites excited by dielectronic recombination have intensities relative to the resonance line that vary as Z^4/T_e , so that, though rather weak for Mg (for example) they are comparable in strength to the resonance line for Fe. The theory has been discussed by Gabriel (1972), and several studies made of temperature variations during flares using particularly iron and calcium lines (see, for example Lemen *et al.* 1984).

For lower- Z ions, the satellites are too weak for very precise temperature determinations, but other line ratios are available. For helium-like stages, the three lines generally prominent in X-ray spectra – the resonance ($1s^2 1S_0 - 1s2p \ ^1P_1$, called here w), intercombination ($1s^2 1S_0 - 1s2p \ ^3P_1$, y), and forbidden ($1s^2 1S_0 - 1s2s \ ^3S_1$, z) lines – show a rather slight temperature dependence through the G ratio, equal to $[I(y) + I(z)]/I(w)$. Atomic calculations at Queen's University, Belfast, for the intensities using the R -matrix code have provided a basis for comparing with FCS observations of the G ratio for various elements. However, in recent work, more sensitive ratios have been explored. The first involves the w , y and z lines of He-like aluminium (Al^{XII}), occurring near 0.78 nm, and the $1s^2 - 1s3p$ line of Mg^{XI} , with wavelength between that of the Al^{XII} y and z lines. The contribution functions (product of fractional ion abundance and collisional excitation rate coefficient) of the Al^{XII} and Mg^{XI} lines have very similar temperature dependence. This means that, though T_e is not too well defined by the Al^{XII} lines through the G ratio, much better constraint is afforded by the presence of the Mg^{XI} line. The work of Bromage *et al.* (1989) shows that the value of T_e can be estimated with a precision of about 1×10^6 K for FCS observations of reasonable quality. Figure 2 shows a synthetic spectrum fitted to an observed spectrum covering the region of the Al^{XII} and Mg^{XI} lines.

Higher- n lines of the He-like stages of various elements are visible in several FCS spectra during flares or even non-flaring but hot active regions, as well as spectra from many previous X-ray spectrometers. The intensity ratios $I(1s^2 - 1snp)/I(w)$ for $n = 3, 4, 5$, etc., have temperature sensitivity that is generally much larger than for the G ratio. R -matrix calculations of the Si^{XIII} ratios for $n = 3-5$ lines and the G ratio have been compared with observations made by the FCS and earlier spectrometers in a study by Keenan *et al.* (1990). The Si^{XIII} $n = 2-5$ lines occur in the region 0.53–0.67 nm. There are very few observations of them – indeed none that covers them all – in the FCS data, and the comparison had to be made with ratios of line ratios that did not prove entirely satisfactory. Possibly there are errors in the calculation of the intensity calibration of this particular channel of the FCS. However, using the data of Walker *et al.* (1974) and Parkinson *et al.* (1978), obtained in a variety of

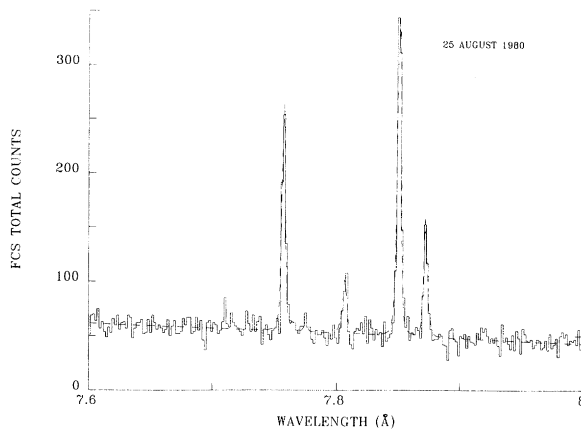


Figure 2. FCS spectrum over the region of the Al^{XII} and Mg^{XI} lines at 0.775–0.79 nm (histogram) compared with a synthetic fitted spectrum (dashed curve). (Unit of wavelength in axis labelling is \AA , where $1 \text{\AA} = 0.1 \text{ nm}$.) The synthetic spectrum was calculated with $T_e = 7.9 \times 10^6 \text{ K}$ and emission measure ($\int N_e^2 dV$) = $8 \times 10^{42} \text{ m}^{-3}$.

conditions (non-flaring active regions, weak and strong flares), Keenan *et al.* deduced values of T_e that were considered very reasonable, so confirming the accuracy of the atomic data.

Much more satisfactory results were obtained with FCS observations of the corresponding ratios in Mg^{XI} (Keenan *et al.* 1991). The observations are more numerous, and there are plenty of non-flaring active-region spectra which have the advantage that there are no significant time variations during the course of the spectral scan. The observed $I(1s^2-1snp)/I(w)$ ($n = 2-4$) ratios, when compared with the theoretical values from the R -matrix calculations, give electron temperatures ($2-4 \times 10^6 \text{ K}$) that are those expected from such regions.

Finally, one should consider the fact that the emitting regions – solar flare or non-flaring active regions – are non-isothermal. Different line ratios give different values of T_e , depending on the ionization stage (though the spread of temperatures is small for active regions). What, then, do the derived temperatures mean? The non-isothermal nature has been expressed by various authors as a temperature-dependent, or ‘differential’, emission measure, so that line flux is given by

$$F = \frac{1}{4\pi r^2} \int_V N_{\text{ion}} N_e C_{12} dV \text{ photons cm}^{-2} \text{ s}^{-1}, \quad (1)$$

where r is the mean Sun–Earth distance, V the emitting volume, the N s number densities of ions and electrons, and C_{12} the rate coefficient of electron collisional excitation from levels 1 to 2, assuming this is the primary means of excitation (this is true except for the case of the dielectronic satellites). Thus,

$$F = \text{const.} \times \int G(T_e) N_e^2 dV, \quad (2)$$

which is transformed to a temperature integral

$$F = \text{const.} \times \int G(T_e) \phi(T_e) dT_e \quad (3)$$

under the conditions stated by Craig & Brown (1976) in their discussion of the problem. In (2) and (3), $G(T_e)$ is the line contribution function

$$G(T_e) = (N_{\text{ion}}/N_{\text{element}}) C_{12}, \quad (4)$$

with N_{element} the number density of ions of all ionization stages, and $\phi(T_e)$ the differential emission measure.

Solution of equation (3) for the functional form of $\phi(T_e)$ using the fluxes of several lines with different $G(T_e)$ s has been attempted for not only X-ray but also ultraviolet lines with a success that is difficult to judge. There are many sources of error (an early discussion of these by Phillips (1975) remains valid), in particular the element abundances to be chosen and the instrument sensitivities. But in the X-ray region, the overriding difficulty is the fact that the $G(T_e)$ functions are extremely broad with temperature, making the problem ill-conditioned. There is little doubt that previous attempts to derive emission measures from FCS data, for example, have little meaning, and not much credence can be given to them.

The problem has more recently been approached in the reverse direction by some authors, *viz.* assume a functional form for $\phi(T_e)$ with adjustable parameters. Temperature-dependent ratios of the type discussed in this section can be derived and compared with observed values, and so parameters or at least a range of them chosen for $\phi(T_e)$. Some success has been achieved using dielectronic satellite ratios by Doschek *et al.* (1990), for instance, and it is hoped that similar treatments will be done for the line ratios discussed here.

4. Element abundances

The ratios of lines due to different elements that coincidentally happen to have the same contribution function $G(T_e)$ should give the ratio of the abundances of the two elements, since all temperature factors involved in the ionization equilibrium and excitation functions will cancel out. This simple idea has had rather limited exploitation so far with the FCS data. One difficulty for flare observations is that it takes a finite time to scan the range between one line and another, during which the flare may significantly vary. The BCS, on the other hand, collects all data within a range simultaneously, and so the data do not suffer this disadvantage. In recent work determinations have been made of the abundance ratios of chlorine to sulphur and of iron to calcium.

Chlorine is an odd- Z , low-abundance element whose solar abundance has only been positively found by spectroscopic means using HCl lines in an infra-red sunspot spectrum (Hall & Noyes 1972), though there are lines in the far-ultraviolet that may possibly be used. The resonance line of the He-like stage (Cl^{XVI}) occurs at 0.444 nm, very near the S^{XV} $1s^2-1s3p$ line (0.430 nm), and their contribution functions are very similar. The spectral region concerned was scanned by the FCS during a large flare on 14 April 1988, and the S^{XV} line was clearly seen. An extremely weak feature also occurs at precisely the same wavelength of the Cl^{XVI} resonance line. On the assumption that this really is the chlorine line, and using atomic data interpolated from R -matrix calculations, Phillips & Keenan (1990) derived the ratio of abundances $A(\text{S})/A(\text{Cl})$ to be 14. By using Meyer's (1985) coronal sulphur abundance relative to hydrogen, the ratio $A(\text{Cl})/A(\text{H})$ is $6 \times 10^{-7} \pm 40\%$, within a factor of two of Hall & Noyes's determination.

The solar abundance of calcium during flares is of great interest at present as the

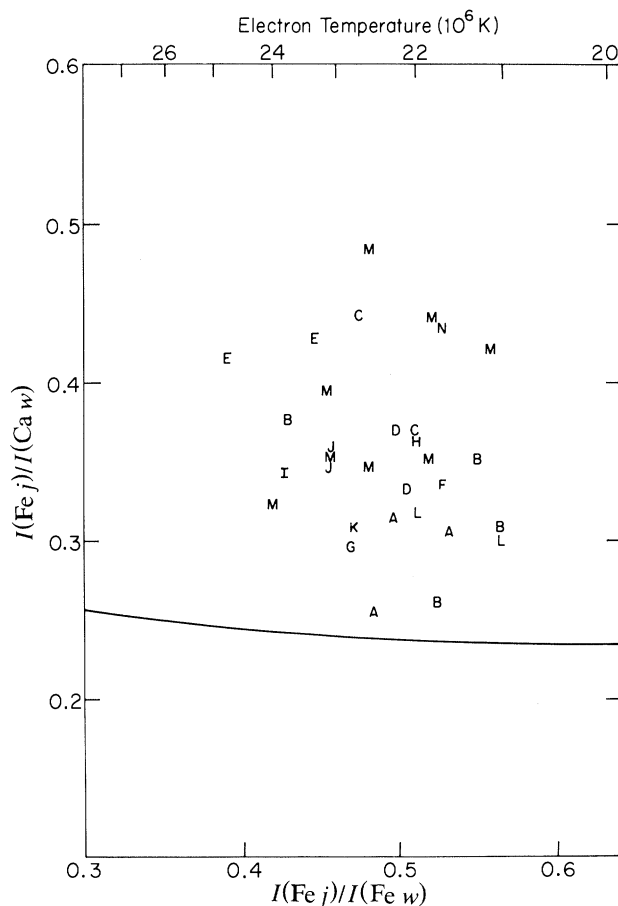


Figure 3. Intensity ratio of $\text{Fe}^{\text{XXIV}} j$ satellite to Ca^{XIX} resonance line $I(\text{Fe}_j)/I(\text{Ca}_w)$ plotted against temperature as represented by the intensity ratio j to the Fe^{XXV} resonance line $I(\text{Fe}_j)/I(\text{Fe}_w)$ (a temperature scale is shown along the top horizontal axis). The theoretical curve is the solid line curve, and the various letters are observed points within individual flares (one letter per flare). The observed points are restricted to the temperature region $21\text{--}25 \times 10^6$ K, corresponding to values of the $I(\text{Fe}_j)/I(\text{Fe}_w)$ ratio of 0.38–0.56.

analysis of BCS data during flares by Sylwester *et al.* (1984) suggests it is variable. This work was based on the intensity of the He-like (Ca^{XIX}) resonance line relative to nearby continuum, which is made up largely of free–free emission. In a recent investigation (Phillips & Feldman 1991), the abundance ratio of iron to calcium was determined for a number of flares from the intensity ratio of an Fe^{XXIV} dielectronic satellite line (referred to as j) to the Ca^{XIX} resonance line, using both BCS and SOLFLEX data. Now the intensity ratio is only constant for a small temperature range, roughly $21\text{--}25 \times 10^6$ K. But values of T_e can be derived from the same dielectronic satellite j to the He-like iron (Fe^{XXV}) resonance line. Thus, line ratio determinations were limited to those occasions when the measured temperature was in the required range. Figure 3 shows a plot of the intensity ratios satellite j to Ca^{XIX} resonance line against temperature as indicated by the ratio of j to the Fe^{XXV} resonance line.

The value $A(\text{Fe})/A(\text{Ca}) = 6.8 \pm 1.0$ was obtained from the SOLFLEX data, 6.0 ± 1.5 from the BCS data. This is fairly similar to other coronal determinations, though it

is substantially less than the photospheric ratio (14) (see Meyer's (1985) tabulation). No significant variation from flare to flare was noted (as can be seen from the errors, which are standard deviations), so that for this result to be compatible with Sylwester *et al.*'s result, both the iron and calcium abundances must vary together.

5. Summary and directions for future work

This review has given some examples of the determinations of physical parameters possible from analysis of X-ray spectra emitted by solar flares and active regions. Electron densities can be found from a rather small number of line ratios, but the range for electron temperature is much greater. The non-isothermal nature of flare and active-region plasma means that such determinations must be folded into differential emission measure ($\phi(T_e)$) analyses, with an assumed form for $\phi(T_e)$ having adjustable parameters. Element abundance ratios can be determined from the intensity ratio of certain lines, depending on the nearness of the form of the appropriate contribution functions. Some items not mentioned here include the determination of departures from ionization equilibrium, using dielectronic satellites that are both dielectronically and collisionally excited, and searching for the presence of non-thermal electrons which may significantly excite certain transitions.

How this spectroscopically derived information can be used as input to models for flares and active regions is a question that has hardly been touched upon hitherto. Flare and active-regions models consist of loop geometries containing hot plasma that is energized by some agent and cooled by radiation, plasma motion, or conduction to the much cooler chromosphere. Often the models have been one dimensional, but there has been increasing sophistication recently. The values for density, temperature and even geometry (e.g. how many loops involved, variation of aspect ratio with loop length) may possibly be specific for certain well-observed flares and active regions, and therefore could be used in model loops in their time development. A most telling observation is the fact that N_e determined from cool ions like Ne^{IX} is high near the maximum of a flare and decreases during the flare decay. It is tempting to think of this indicating a loop contraction, perhaps by a pinch effect, but it may be that the emitting region simply moves to a high, less dense region as the flare progresses. This question is among those that could be answered by linking spectroscopic data with models.

References

- Arnaud, M. & Rothenflug, R. 1985 An updated evaluation of recombination and ionization rates. *Astron. Astrophys. Suppl. Ser.* **60**, 425–457.
- Bhatia, A. K., Fawcett, B. C., Lemen, J. R., Mason, H. E. & Phillips, K. J. H. 1989 A comparison of theoretical and solar-flare intensity ratios for the Fe^{XIX} X-ray lines. *Mon. Not. R. astr. Soc.* **240**, 421–444.
- Bromage, B. J. I., Phillips, K. J. H., Keenan, F. P. & McCann, S. M., 1989 Use of Al^{XII} and Mg^{XI} lines as solar plasma diagnostics. *Solar Phys.* **124**, 289–302.
- Craig, I. J. D. & Brown, J. C. 1976 Fundamental limitations of X-ray spectra as diagnostics of plasma temperature structure. *Astron. Astrophys.* **49**, 239–250.
- Doschek, G. A., Feldman, U., Landecker, P. B. & McKenzie, D. L. 1981 High resolution solar flare X-ray spectra: the temporal behavior of electron density, temperature, and emission measure for two class M flares. *Astrophys. J.* **249**, 372–382.
- Doschek, G. A., Fludra, A., Bentley, R. D., Phillips, K. J. H., Lang, J. & Watanabe, T. 1990 On the dependence of solar flare X-ray spectra line intensity ratios of highly ionized sulfur, calcium
- Phil. Trans. R. Soc. Lond. A* (1991)

- and iron on electron temperature, differential emission measure, and atomic physics. *Astrophys. J.* **358**, 665–675.
- Feldman, U., Cheng, C.-C. & Doschek, G. A. 1982 Observational constraints for a theoretical model describing the soft X-ray flare. *Astrophys. J.* **255**, 320–326.
- Gabriel, A. H. 1972 Dielectronic satellite spectra for highly charged helium-like ion lines. *Mon. Not. R. astr. Soc.* **160**, 99–115.
- Gabriel, A. H. & Jordan, C. 1969 Interpretation of solar helium-like ion line intensities. *Mon. Not. R. astr. Soc.* **145**, 241–248.
- Hall, D. N. B. & Noyes, R. W. 1972 The identification of the 1-0 and 2-1 bands of HCl in the infrared sunspot spectrum. *Astrophys. J.* **175**, L95–L97.
- Keenan, F. P., Harra, L. K. & Phillips, K. J. H. 1991 Mg^{XI} emission line ratios in solar active regions. *Astrophys. J.* (In the press.)
- Keenan, F. P., McKenzie, D. L., McCann, S. M. & Kingston, A. E. 1987 Ne^{IX} emission-line ratios in solar active regions. *Astrophys. J.* **318**, 926–929.
- Keenan, F. P., McCann, S. M. & Phillips, K. J. H. 1990 The 1^S–*n*1^P/1^S–2¹P emission-line ratios in Si^{XIII} as electron temperature diagnostics for solar flares and active regions. *Astrophys. J.* **363**, 310–314.
- Lemen, J. R., Phillips, K. J. H., Cowan, R. D., Hata, J. & Grant, I. P. 1984 Inner-shell transitions of Fe^{XXIII} and Fe^{XXIV} in the X-ray spectra of solar flares. *Astron. Astrophys.* **135**, 313–324.
- Meyer, J.-P. 1985 Solar-stellar outer atmospheres and energetic particles and galactic cosmic rays. *Astrophys. J. Suppl.* **57**, 173–204.
- Parkinson, J. H., Wolff, R. S., Kestenbaum, H. L., Ku, W. H.-M., Lemen, J. R., Long, K. S., Novick, R., Suozzo, R. J. & Weisskopf, M. C. 1978 Silicon X-ray line emission from solar flares and active regions. *Solar Phys.* **60**, 123–136.
- Phillips, K. J. H. 1975 Temperature dependence of emission measure in solar X-ray plasmas. I. Nonflaring active regions. *Astrophys. J.* **199**, 247–254.
- Phillips, K. J. H. & Feldman, U. 1991 The iron-to-calcium abundance ratio in the 20-million-degree plasma of medium and large solar flares. *Astrophys. J.* (In the press.)
- Phillips, K. J. H. & Keenan, F. P. 1990 Solar chlorine abundance from an X-ray flare spectrum. *Mon. Not. R. astr. Soc.* **245**, 4P–6P.
- Phillips, K. J. H., Leibacher, J. W., Wolfson, C. J., Parkinson, J. H., Fawcett, B. C., Kent, B. J., Mason, H. E., Acton, L. W., Culhane, J. L. & Gabriel, A. H. 1982 Solar flare X-ray spectra from the *Solar Maximum Mission* Flat Crystal Spectrometer. *Astrophys. J.* **256**, 774–787.
- Phillips, K. J. H., Lemen, J. R., Cowan, R. D., Doschek, G. A. & Leibacher, J. W. 1983 Inner-shell transitions in Fe^{XIX}–Fe^{XXII} in the X-ray spectra of solar flares and tokamaks. *Astrophys. J.* **265**, 1120–1134.
- Sylwester, J., Lemen, J. R. & Mewe, R. 1984 Variation in observed coronal calcium abundance of X-ray flare plasmas. *Nature* **310**, 665–666.
- Walker, A. B. C., Ruge, H. R. & Weiss, K. 1974 Relative coronal abundances derived from X-ray observations. *Astrophys. J.* **188**, 423–440.

Discussion

A. FLUDRA (*University College, London, U.K.*). A paper by Fludra *et al.* (*Adv. Space Res.* **11**, 1155 (1991)) gives values of iron abundances relative to hydrogen and also relative to calcium for 12 flares observed by *SMM*-BCS. These values are derived using a new method based on the multi-temperature analysis. This method is more general than using a ratio of two lines in a restricted temperature range. Derived iron abundances depend on the choice of ionization balance calculations. When the ionization balance for iron published by Arnaud & Rothenflug is used, the value of iron abundance relative to calcium is roughly equal to 10 in a sample of seven flares and it is between 12 and 15 for five other flares. After an empirical correction is made

to the ionization balance for iron to remove a marked temperature dependence of the abundances, the abundance ratios of iron to calcium vary from 10 to 25 between flares.

K. J. H. PHILLIPS. We (Phillips & Feldman 1991) found from our sample of 29 flares from two spectrometers on separate spacecraft a fairly constant iron-to-calcium abundance ratio. Our method used a line-to-line ratio which ought to be more direct than using the continuum. It is worth pointing out that any method is at the mercy of atomic data inaccuracies, particularly those in ionization-equilibrium ratios.